Papers from the GEOPHYSICAL LABORATORY
Carnegie Institution of Washington NO. 2041

ACS SYMPOSIUM SERIES 351

Chemistry of High-Temperature Superconductors

David L. Nelson, EDITOR
Office of Naval Research

M. Stanley Whittingham, EDITOR
Schlumberger-Doll Research

Thomas F. George, EDITOR
State University of New York at Buffalo

Developed for symposia sponsored
by the Divisions of Inorganic Chemistry
and Physical Chemistry
at the 194th Meeting
of the American Chemical Society,
New Orleans, Louisiana,
August 30-September 4, 1987

American Chemical Society, Washington, DC 1987

Chapter 16

Oxygen-Defect Perovskites and the 93-K Superconductor

N. L. Ross, R. J. Angel, L. W. Finger, R. M. Hazen, and C. T. Prewitt

Geophysical Laboratory, Carnegie Institution of Washington, 2801 Upton Street, NW, Washington, DC 20008

The structure of the tetragonal phase of $YBa_2Cu_3O_6$ is presented and discussed in relation to both the orthorhombic structure of the 93K superconductor and the known structures of other oxygen defect perovskites. The reduction of oxygen content from the ideal ABO_3 stoichiometry of perovskites reduces the primary coordination of both the A and B cation sites. In particular, with decreasing oxygen content the octahedral B site first becomes a square-based pyramid (5 coordinating oxygens), then square-planar or pseudo-tetrahedral (4) and finally linearly coordinated by two oxygens. Such behaviour is especially prevalent in those phases containing variable oxidation state transition-metal cations such as Cu, Mn, and Fe, which can be accommodated in these variable-coordination sites. The superconducting phase $Ba_2YCu_3O_{7-x}$ is a defect perovskite which exhibits many of these structural variations. Samples with high oxygen content (x=0) have two types of oxygen vacancies. One is the removal of all the oxygen atoms from layers level with the Y atoms (in A sites). This reduces the coordination of the two adjacent layers of Cu sites to 5-fold square-based pyramids. The second set of oxygen vacancies is adjacent to the other copper atoms, reducing their coordination to square-planar. Further reduction of the oxygen content to O_6 (x=1) results in the removal of oxygen from this square-planar array to produce linear O-Cu-O groups; these remaining oxygens also form the apices of the square-based pyramids.

The discovery by Wu et al. (1) of superconductivity at 93K in a mixed-phase sample in the Y-Ba-Cu-O system has stimulated an unprecedented amount of research effort directed at solving the structures of the phase(s) responsible for superconductivity. In this paper we will present the results of the first single-crystal structure analyses of the phases present in these samples to be carried out (2), and then review the additional structural information now available in relation to the previously determined structures of other oxygen defect perovskites.

Y_2BaCuO_5 Structure

The polycrystalline sample in which superconductivity at temperatures in excess of 93K was first observed consisted of two major phases. Electron microprobe analyses indicated that a green transparent phase, which comprised the majority of the early samples, contained Ba, Cu and Y in the ratios 1:1:2. A single crystal diffraction study and structure solution by direct methods indicated that this green phase has an ideal composition Y_2BaCuO_5, and a structure similar to that reported on the basis of powder diffraction (3). Crystallographic data for this structure are reported in Table I.

0097-6156/87/0351-0164$06.00/0

Table I. Crystallographic data for Y_2BaCuO_5

Space group: Pbnm (determined by diffraction absences and structure determination)
Unit Cell data: a=7.123 Å, b=12.163 Å, c=5.649 Å, V_{cell} = 489.4 Å^3, Z = 4, ρ_{calc} = 6.22

		Positional Parameters		
Atom	Mult.	x/a	y/b	z/c
Ba	4	0.93	0.90	0.25
Y1	4	0.12	0.29	0.25
Y2	4	0.40	0.07	0.25
Cu	4	0.71	0.66	0.25
O1	8	0.16	0.43	0.00
O2	8	0.36	0.23	0.50
O3	4	0.03	0.10	0.25

This structure, shown in Figure 1, is unusual in that it contains Y_3+ in trigonal pyramid coordination, as well as copper in capped square-planar coordination (alternatively described as a square-based pyramid), the latter feature being shared with the structure of the superconducting phase.

$YBa_2Cu_3O_{7-x}$

Structure Analysis. The superconducting phase comprised about one-third of the earliest samples received from the University of Houston. Electron microprobe analyses indicated a cation ratio of Ba:Cu:Y of 2.1:2.9:1.0. Unit cell parameters were determined on a number of different crystals, and indicated that the unit cell was tetragonal with a=3.859 Å, c=3.904 Å. Some crystals in later batches deviated from exact tetragonal symmetry, indicating that ordering within the structure was reducing the symmetry to orthorhombic. X-ray diffraction studies showed that single crystals had 4/mmm Laue symmetry, and diffraction symbol 4/mmmP..., allowing as possible space groups P422, P4mm, P$\bar{4}$m2, P$\bar{4}$2m, and P4/mmm. With all of the cations within the unit cell occupying the special positions of the perovskite structure, these four possible space groups are only distinguished by the position of the oxygen atoms, which are comparatively weak scatterers of X-rays. Thus an N(z) test of X-ray diffraction data is not a reliable indicator of the presence or absence of a center of symmetry in the structure. A combination of direct methods and least squares refinements was used to solve the structure, and crystallographic data are reported in Table II for the two most likely space groups.

The structure of this tetragonal phase is shown in Figure 2a and, like a number of oxygen-defect perovskites discussed below, exhibits variable co-ordination of cations by the oxygen anions. The key to understanding the structure lies in the ordering of the barium and yttrium cations over the 'A' sites of the perovskite structure. In cubic and metrically cubic perovskites these sites are coordinated to 12 anion positions at a distance of $\sqrt{2}a_c$. However, Y^{3+} is a much smaller cation than Ba^{2+}, (Shannon-Prewitt radii of 1.02 Å and 1.42-1.60 Å respectively (4)), and the oxygens surrounding the yttrium sites can be thought as being 'drawn in' towards the central Y site. As a consequence the ideally cubic sub-cell around the Y site at 1/2,1/2,1/2 is shortened along the c axis of the structure, while the cells around the Ba sites are expanded. This shortening of the central sub-cell of the structure results in a distance of 3.30 Å between pairs of Cu2 sites at 0,0,0.36 and 0,0,0.64. Oxygen anions are therefore excluded from the site at 0,0,1/2 as their presence would require Cu-O distances of 1.65 Å. Thus we see that this phase is required to have at least one vacant oxygen site by crystal chemical constraints. The resulting coordination of the Cu2 site can be described as slightly distorted versions of a square-based pyramid, or a capped square-planar array.

In contrast to the vacancies at z=1/2, the oxygen sites at z=0 are not required to be vacant by crystal chemistry. It is these sites that show the variable occupancy that gives rise to the variable stoichiometry and complicated structural phase relations to be discussed below. In our

tetragonal phase however these sites are also almost completely devoid of scattering density, indicating that the oxygen content of this material is very close to O_6. The coordination of the Ba sites is accordingly reduced from the value of twelve for an ideal structure, to eight. The off center distribution of the remaining oxygens (Figure 2a) accounts for the displacement of the barium atoms from an ideal z-coordinate of 1/6 to the observed z=0.19. The Cu1 sites are also reduced in coordination, from six in an ideal perovskite, to two. The presence of this linear O-Cu-O group could account for some of the similarities to cuprite, Cu_2O, noted in the Raman spectra of these samples (5).

Table II. Crystallographic data for $YBa_2Cu_3O_6$

Unit cell parameters: a=b=3.859 Å, c=11.71 Å, V_{cell} = 174.4 Å^3, ρ_{calc} = 6.19

Positional Parameters

	$P\bar{4}m2$				P4/mmm			
Atom	Mult.	x/a	y/b	z/c	Mult.	x/a	y/b	z/c
Ba	2	0.50	0.50	0.19	2	0.50	0.50	0.19
Y	1	0.50	0.50	0.50	1	0.50	0.50	0.50
Cu1	1	0.00	0.00	0.00	1	0.00	0.00	0.00
Cu2	2	0.00	0.00	0.36	2	0.00	0.00	0.36
O1	2	0.50	0.00	0.38	4	0.50	0.00	0.38
O2	2	0.50	0.00	0.61				
O3	2	0.00	0.00	0.15	2	0.00	0.00	0.15

Phase transitions and Average Structures. It is clear from the large quantity of structural information now available for the $YBa_2Cu_3O_{7-x}$ compound that there are a number of distinct structures that differ in structural detail. Both the local structure and the apparent long-range structure of these materials are determined by the thermal history and the oxygen content of the structure, which appears to vary between O_6 and O_7, although there is one report (Beyers, R. et al., Appl. Phys. Letts., submitted) of an $O_{7.4}$ composition. At the lowest oxygen contents, O_6, to which the structure reported above approximates, the structure is truly tetragonal both on local and long-range scales. This is because both of the oxygen sites at z=0 (1/2,0,0 and 0,1/2,0) are vacant, and there is nothing to distinguish the *a* and *b* axes of the unit cell. When the oxygen content of the structure is increased these sites may either be equally and partially occupied, or one may be occupied in preference to the other. To take an end-member case, with an oxygen content of O_7 the crystal may be tetragonal with both of these oxygen sites being half occupied, or one may be fully vacant and the other fully occupied. In the latter case the *a* and *b* axes are now distinguishable, and the structure is orthorhombic (6) with the Cu1 sites in square planar coordination (Figure 2b).

It is also important to distinguish the type of disorder within the structure, which may be dynamic or static. Static disorder is the apparent random occupancy of one site or the other by oxygen atoms, while dynamic disorder involves the rapid exchange of oxygen atoms between the two sites. In both cases the average structure 'seen' by X-ray or neutron single crystal diffraction techniques remains tetragonal. On the other hand, if the distribution is static, a powder diffraction experiment will result in the true symmetry independent of the domain distribution, provided that the domains are larger than the correlation length. It is for this reason that powder diffraction techniques have been successful in determining the orthorhombic structure (7; Beech, F. et al., Phys. Rev. Letts. , submitted; Beno M.A. et al., Appl. Phys. Letts. , submitted). However, in the static case local ordering of the oxygens and vacancies may give rise to orthorhombic domains within the crystals, which then appear to be (110) twins (8; Beyers, R. et al., Appl. Phys. Letts., submitted; Sueno, S. et al., Jap. J. Appl. Phys., in press). The size of these domains is clearly dependent upon both the oxygen content and upon the

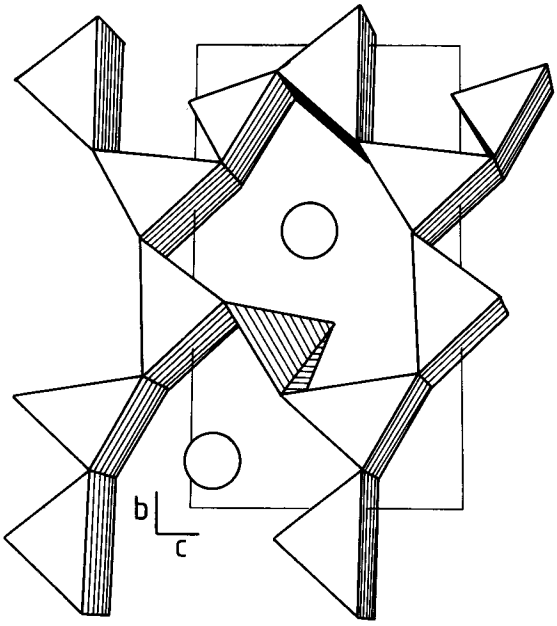

Figure 1. Polyhedral representation of the Y_2BaCuO_5 structure. The large circles represent Ba sites.

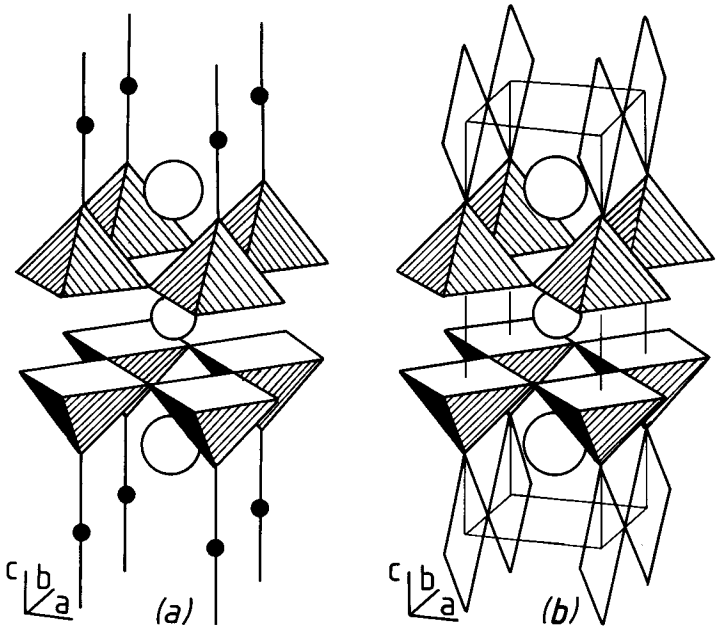

Figure 2. Polyhedral representation of (a) $YBa_2Cu_3O_6$ and (b) $YBa_2Cu_3O_7$. The large circles represent Ba sites, intermediate circles Y sites.

thermal history of the samples, and in the limit single orthorhombic crystals with space group Pmmm can be grown.

Dynamic disordering is responsible for the phase transition between the low temperature orthorhombic structure and a high temperature tetragonal phase in which all of the anion sites at z=0 are statistically and equally occupied by oxygen atoms. The wide range of reported temperatures for this transition (Schuller, I.K. et al., Solid State Comm., submitted; Sueno, S. et al., Jap. J. Appl. Phys. , in press) clearly represent a true variation of the transition temperature with oxygen content and the scale of ordering within the structure (9). The space group of this dynamically disordered phase must be a tetragonal supergroup of the Pmmm symmetry of the orthorhombic phase - and is therefore P4/mmm. However, this does not necessarily imply that a structure with an oxygen content of O_6 must possess this space group. Indeed, the displacements of the fully occupied anion sites are quite likely to be different in the two cases, and could lead to different space groups for the disordered phase and the O_6 tetragonal phase. It should also be noted that neither the orthorhombic - tetragonal phase transition, nor the varying scales of ordering within the orthorhombic phase, give rise to a structure similar to that proposed for $La_3Ba_3Cu_6O_{14}$ (10), as suggested recently by some groups (11,12). In fact, a review of the available data (Ross, N.L. et al., Nature, submitted) suggests that $La_3Ba_3Cu_6O_{14}$ actually possesses the tetragonal structure reported here for the superconductor.

Oxygen-Defect Perovskites

We have now discussed in detail the structure of $YBa_2Cu_3O_{7-x}$ with respect to the thermal history and oxygen content of the phase. These two variables determine the local structure and apparent long-range structure present in the phase, that is, the distribution of oxygen vacancies in the structure. Since $YBa_2Cu_3O_{7-x}$ is a true derivative of the ideal perovskite structure, a comparison of this compound with other oxygen-defect perovskites provides a basis from which to gain a greater understanding of this class of materials. In the following sections, the structure of the high T_c superconductor will be discussed in relation to other oxygen-defect perovskites derived from removal of oxygen atoms from the ideal perovskite prototype.

Polyhedral Elements . The perovskite prototype, ABO_3, consists of a framework of corner-linked BO_6 octahedra extending infinitely in three dimensions, with a large A cation in 12-fold coordination occupying the cavity created by the linkage of eight octahedra at the corners of a cube outlining the unit cell of the structure. The reduction of oxygen content from the ideal ABO_3 stoichiometry by substitution of low-valence metal cations for high-valence metal cations reduces the primary coordination of the A and B cation sites. With decreasing oxygen content, the octahedral B site first becomes a capped square plane or square-based pyramid with five coordinating oxygen atoms. $CaMnO_{2.5}$(13,14) and $SrMnO_{2.5}$(15), for example, have five-coordinate Mn^{3+} cations with approximately square-pyramidal coordination. The Cu2 atoms in both the orthorhombic and tetragonal structures of the high T_c superconductor are also in square-pyramidal coordination (Figure 2). Further removal of oxygen atoms results in cations that are in 4-fold coordination. We have already discussed the example of the $Cu1^{2+}$ atoms in square-planar coordination in the orthorhombic structure of the high T_c superconductor (Figure 2b). There are, however, examples of metal cations that prefer tetrahedral coordination. $Ca_2Fe_2O_5$(16) and $Sr_2Fe_2O_5$(17) crystallize in structures closely related to that of brownmillerite, Ca_2FeAlO_5 (18). In all of these structures one half of the Fe^{3+} cations are in tetrahedral coordination and one half are in octahedral coordination (Figure 3). Finally, the oxygen content may be reduced even further, resulting in B sites that are linearly coordinated by two oxygens. To the authors' knowledge, the coordination of the Cu1 sites in the tetragonal high T_c superconductor (Figure 2a) is the first example of an oxygen-defect perovskite with this type of coordination. It is also the most oxygen-deficient perovskite ($ABO_{2.0}$) known.

From the examples given above, it is apparent that the coordination geometry adopted by the metal cations in the B-sites depends on the particular transition metal cations present in the structure. Mn^{3+} prefers square pyramidal coordination while Cu^{2+} is found in both square pyramidal and square planar coordination. Fe^{3+}, on the other hand, is commonly found in tetrahedral and octahedral coordination, but not in square pyramidal coordination. Thus although $CaMnO_{2.5}$ and $SrFeO_{2.5}$ have the same oxygen stoichiometry, they crystallize with totally different structures.

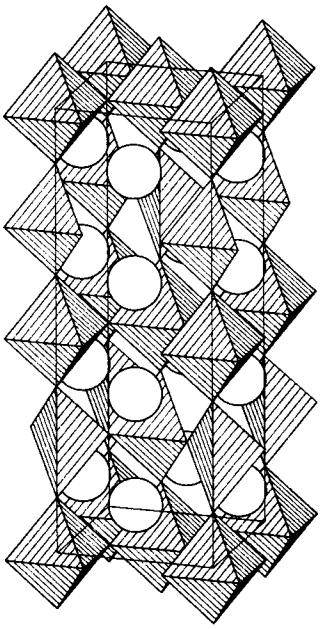

Figure 3. Polyhedral representation of the brownmillerite structure.

Oxygen Vacancy Arrangements. The structure of individual oxygen-defect perovskites therefore depends not only on the overall oxygen content of the structure, but also on the polyhedral coordination preference of the metal cations present in the structure. This section will focus on the oxygen vacancy arrangements present in specific oxygen-defect perovskites resulting from organization of the polyhedral units.

The structures of $CaMnO_{2.5}$ and $SrMnO_{2.5}$ are characterized by orthorhombic cells with $a \cong \sqrt{2}a_c$, $b \cong 2\sqrt{2}a_c$ and $c \cong a_c$. The host lattice is derived from the perovskite prototype by ordering of oxygen vacancies on the (001) planes of the cubic perovskite that form pseudo-hexagonal tunnels running along $[001]_c$. Every second $[110]_c$ row of oxygen sites has oxygen vacancies alternating with oxygen atoms. Successive defect rows are displaced by $a/2$, so as to generate square-based pyramidal coordination for all of the Mn^{3+}. The Ca^{2+} and Sr^{2+} cations, which are surrounded by 10 rather than 12 nearest neighbors, are believed to play a secondary role in maintaining the parallel channels of oxygen vacancies.

The structures of $CaFeO_{2.5}$ and $SrFeO_{2.5}$, on the other hand, are characterized by orthorhombic cells with $a=c \cong \sqrt{2}a_c$ and $b \cong 4a_c$. Layers of perovskite-like FeO_6 octahedra alternate with (001) layers in which two oxygen atoms have been removed from every octahedron. As with the manganate structures, oxygen vacancies propagate along $[110]_c$. Unlike the manganate structures, every oxygen atom along particular $[110]_c$ strings is missing, leaving Fe^{3+} with only four nearest neighbors. The ordering of vacancy strings is such that half the iron atoms remain octahedrally coordinated and half are tetrahedrally coordinated. The Ca^{2+} and Sr^{2+} cations occupy the large interstices between the layers, surrounded by eight nearest neighbors.

Tofield et al.(19) proposed a model for oxygen vacancy ordering in $SrFeO_{2.75}$ which is of interest because of its close relationship to the structures described above. This model structure has either orthorhombic or body-centered tetragonal symmetry with cell dimensions of $a=c \cong 2\sqrt{2}a_c$ and $b \cong 2a_c$. Similar to the ferrite and manganate oxygen-defect perovskites, the oxygen vacancies in $SrFeO_{2.75}$ also propagate along $[110]_c$. Every other oxygen, however, is missing along these $[110]_c$ vacancy strings as in $CaMnO_{2.5}$ and $SrMnO_{2.5}$, but not in $CaFeO_{2.5}$ and $SrFeO_{2.5}$. The manganate structure can, in fact, be simply derived from the structure proposed for $SrFeO_{2.75}$. Let A represent one of the oxygen-vacancy strings along $[110]_c$ which has the oxygen(O)/vacancy(v) arrangement, ...v-O-v-O-v..., and let B represent a $[110]_c$ string with no vacancies, ...O-O-O-O-O..., and let C represent a string with the pattern,...O-v-O-v-O..., in which the vacancies are displaced relative to A. Adjacent $[110]_c$ strings in $CaMnO_{2.5}$ structure have the pattern, ...ABCBABCBABCBA..., and the corresponding pattern in the model structure proposed for $SrFeO_{2.75}$ is ...ABBBABBBABBBA... . Thus the structure of $CaMnO_{2.5}$ can be derived directly from the proposed model upon substitution of strings with oxygen vacancies (C) for every second fully-occupied $[110]_c$ oxygen chain (B). The $SrFeO_{2.5}$ structure, however, cannot be directly derived from the proposed structure without involving rearrangement of the oxygen atoms and vacancies concommittant with removal of oxygen atoms.

In Tofield et al.'s model for $SrFeO_{2.75}$, half of the iron atoms remain in octahedral coordination and half are in five-fold coordination. In view of the observed preference of Fe^{3+} for tetrahedral and octahedral coordination, and of Mn^{3+} for pyramidal coordination, we would expect that this proposed structure type would be more appropriate for manganate $O_{2.75}$ perovskites than for those containing iron. Indeed, Grenier et al.(20) have reported a ferrite with the same oxygen stoichiometry, $Ca_4Fe_2Ti_2O_{11}$, which has a structure related to that of brownmillerite, but with a 1:3 ratio of tetrahedral to octahedral layers.

The oxygen vacancies in the oxygen-defect perovskites described above all propagate along the $[110]_c$ of the cubic perovskite cell. The arrangement of the oxygen vacancies at z=0 within the orthorhombic structure of the high T_c superconductor follows a similar pattern. However, as a consequence of the low oxygen content of the unit cell ($O_{2.33}$ on an O_3 basis) every one of these [110] rows has alternate occupied and vacant sites. As in $CaMnO_{2.5}$ and $SrMnO_{2.5}$ each successive defect containing row is displaced relative to its neighbours. In $YBa_2Cu_3O_7$ this arrangement results in the square planar coordination of the Cu1 sites. The total absence of oxygen from the z=1/2 planes, however, is a new perovskite feature and, as discussed above, is a crystal-chemical consequence of the ordering of Ba^{2+} and Y^{3+} on the A sites.

Static and Dynamic Ordering. As with the 93 K superconductor, the local and long-range ordering present in oxygen-defect perovskites is controlled, in large part, by the oxygen content of the samples. This is illustrated very clearly by the work of Grenier et al.(20,21). Grenier et al.(21) proposed a general model for oxygen ordering in intermediate compositions between

$Ca_2Fe_2O_5$ and ABO_3 (A=Ca,Sr,Ba,Y,La,Gd; B=Fe,Ti). Based on the relationship between the brownmillerite structure and the perovskite structure, they proposed that the structures of intermediate compositions would consist of a succession of perovskite-like sheets of corner-linked $[BO_6]$ octahedra separated by sheets of $[BO_4]$ tetrahedra. Grenier et al.(20) found, however, in the $Ca_2Fe_{2x}Ti_{2-2x}O_{6-x}$ solid solutions ($0 \leq x \leq 1$) that ordered structures with a succession of octahedral and tetrahedral sheets exist only for compositions with $0.50 \leq x \leq 1$. The most oxygen-deficient endmember, $Ca_2Fe_2O_5$, crystallizes with the brownmillerite structure which has a 1:1 ratio of tetrahedral to octahedral layers. With increasing oxygen content up to x=0.5, they observed three more structures with ordered oxygen vacancies, $Ca_5[Fe_2Ti]_O[Fe_2]_TO_{13}$, $Ca_3[FeTi]_O[Fe]_TO_8$ and $Ca_4[FeTi_2]_O[Fe]_TO_{11}$. These compounds have ratios of octahedral to tetrahedral sheets of 3:2, 2:1 and 3:1, respectively, thus corroborating their model. Near compositions of x=0.5, ordered microdomains appeared which later gave rise to a long-range ordered structure. For x less than 0.5, the average structure determined by x-ray diffraction had cubic symmetry, corresponding to a disordered perovskite structure. The Mössbauer spectra, however, showed that some of the Fe^{3+} cations were still in tetrahedral coordination suggesting that, even in the absence of superlattice ordering, the oxygen vacancies still tend to combine in pairs with Fe^{3+} inducing a change from octahedral to tetrahedral coordination.

In addition to these examples of static ordering of oxygen and vacancies, even in structures without long-range order, it is possible for these structures to undergo dynamic disordering of oxygens and vacancies to produce a structure with higher symmetry. Such a transition has been observed in both $YBa_2Cu_3O_{7-x}$ and in $Sr_2Fe_2O_5$ (22). The low temperature form of the latter has the orthorhombic symmetry of the brownmillerite structure with statically ordered oxygen vacancies. Above 700°C, the phase has the cubic symmetry of an oxygen-deficient perovskite with all anion sites equally and statistically occupied by oxygen atoms. Given that the transition to a disordered cubic structure involves a complete randomization of the oxygen sublattice, substantial disorder would be expected to exist just below the transition temperature. Similar order-disorder transitions would be expected to occur at high temperatures in intermediate structures in the $CaFeO_{2.5}$ - $CaTiO_3$ system since they have similar oxygen vacancy ordering schemes.

Conclusions

Our review of the structural variations found in a number of oxygen defect perovskites has demonstrated that the structure of the high T_c superconductor $YBa_2Cu_3O_{7-x}$ has both some normal and unusual crystal chemical features. The ordering of oxygen atoms around the Cu1 sites is similar to patterns found in a wide variety of other perovskite derivatives, and gives rise to similar order-disorder behaviour. The novel feature of the oxygen-vacancy ordering arises as a consequence of the ordering of Ba^{2+} and Y^{3+} over the A sites. This ordering forces a complete plane of oxygen atoms to be missing from the structure, but with the interesting result that the B site coordination of Cu2 is pyramidal, a coordination found in other oxygen-defect perovskites.

Acknowledgments

This work has been supported in part by National Science Foundation grants EAR8419982, EAR8608941 and EAR8319504, by a NATO fellowship to RJA, and by the Carnegie Institution of Washington.

Literature Cited

1. Wu, M.K.; Ashburn, J.R.; Torng, C.J.; Hor, P.H.; Meng, R.L.; Gao, L.; Huang, Z.J.; Wang, Y.Q.; Chu, C.W. Phys. Rev. Letts. 1987, 58, 908-910.
2. Hazen, R.M.; Finger, L.W.; Angel, R.J.; Prewitt, C.T.; Ross, N.L.; Mao, H.K.; Hadidiacos, C.G.; Hor, P.H.; Meng, R.L.; Chu, P.W. Phys. Rev. B 1987, 35, 7238-7241.
3. Michel, C.; Raveau, B. J. Solid State Chem. 1982, 43, 73-80.
4. Shannon, R.D.; Prewitt, C.T. Acta Cryst. 1969, B25, 925-946.
5. Hemley, R; Mao, H.K. Phys. Rev. Letts. 1987, 58, 2340-2342.
6. Siegrest, T.; Sunshine, S; Murphy, D.W.; Cava, R.J.; Zahurak, S.M. Phys. Rev. B 1987, 35, 7137-7139.

7. Capponi, J.J.; Chaillout, C.; Hewat, A.W.; Lejay, P.; Marezio, M.; Nguyen, N.; Raveau, B.; Soubeyroux, J.L.; Tholence, J.L.; Tournier, R. Europhys. Letts. 1987, 3, 1301-1308.
8. LePage, Y.; McKinnon, W.R.; Tarascon, J.M.; Greene, L.H.; Hull, G.W.; Hwang, D.W. Phys. Rev. B. 1987, 35, 7245-7248.
9. Strobel, P.; Capponi, J.J.; Chaillout, C.; Marezio, M.; Tholence, J.L. Nature 1987, 327, 306-308.
10. Er-Rakho, L.; Michel, C.; Provost, J.; Raveau, B.J. J. Solid State Chem. 1981, 37, 151-157.
11. Hirabayashi, M.; Ihara, H.; Terada, N.; Senzaki, K.; Hayashi, K.; Waki, S.; Murata, K.; Tokumoto, M.; Kimura, Y. Jap. J. Appl. Phys. 1987, L454-455.
12. Qadri, S.B.; Toth, L.E.; Osofsky, M.; Lawrence, S.; Gubser, D.U.; Wolf, S.A. Phys. Rev. B 1987, 35, 7235-7237.
13. Poeppelmeier, K.R.; Leonowicz, M.E.; Longo, J.M. J. Solid State Chem. 1982, 44, 89-98.
14. Poeppelmeier, K.R.; Leonowicz, M.E.; Scanlon, J.C.; Longo, J.M. J. Solid State Chem. 1982, 45, 71-79.
15. Caignaert, V.; Nguyen, N.; Hervieu, M.; Raveau, B. Mat. Res. Bull. 1985, 20, 479-484.
16. Hughes, H.; Ross, P.; Goldring, D.C. Min. Mag. 1967, 36, 280-291.
17. Greaves, C.; Jacobson, A.J.; Tofield, B.C.; Fender, B.E.F. Acta. Cryst. 1975, B31, 641-646.
18. Colville, A.A.; Geller, S. Acta. Cryst. 1971, B27, 2311-2315.
19. Tofield, B.C.; Greaves, C.; Fender, B.E.F. Mat. Res. Bull. 1975, 10, 737-746.
20. Grenier, J.C.; Menil, F.; Pouchard, M.; Hagenuller, P. Mat. Res. Bull 1978, 13, 329-337.
21. Grenier, J.C.; Darriet, J.; Pouchard, M.; Hagenmuller, P. Mat. Res. Bull. 1976, 11, 1219-1226.
22. Shin, S.; Yonemura, M.; Ikawa, H. Mat. Res. Bull. 1978, 13, 1017-1021.

RECEIVED July 6, 1987

Reprinted from ACS SYMPOSIUM SERIES No. 351
Chemistry of High-Temperature Superconductors
David L. Nelson, M. Stanley Whittingham, and Thomas F. George, Editors